


BIOFUNCTIONALIZATION THROUGH THE USE OF POLYELECTROLYTE MICELLES AND ERYTHROCYTES

JUSTYNA WIĘCEK-CHMIELARZ^{1*} , WOJCIECH KAJZER² ,
JOANNA CHWIEJ³ , ALEKSANDRA WILK³ ,
ZUZANNA ZAJĄC^{1,4} , ROMAN MAJOR^{1*} 

¹ INSTITUTE OF METALLURGY AND MATERIALS SCIENCE, POLISH ACADEMY OF SCIENCES, 25 REYMONTA ST., 30-059 KRAKOW, POLAND

² DEPARTMENT OF BIOMATERIALS AND MEDICAL DEVICES ENGINEERING, FACULTY OF BIOMEDICAL ENGINEERING, SILESIAN UNIVERSITY OF TECHNOLOGY, ROOSEVELTA 40 ST., ZABRZE 41-800, POLAND

³ AGH UNIVERSITY OF KRAKOW, FACULTY OF PHYSICS AND APPLIED COMPUTER SCIENCE, DEPARTMENT OF MEDICAL PHYSICS AND BIOPHYSICS, AL. A. MICKIEWICZA 30, 30-059 KRAKOW, POLAND

⁴ DEPARTMENT OF EXPERIMENTAL MECHANICS AND BIOMECHANICS, FACULTY OF MECHANICAL ENGINEERING, CRACOW UNIVERSITY OF TECHNOLOGY, 37 JANA PAWŁA II AV., 31-864 KRAKOW, POLAND

*E-MAIL: WIECEK.J@IMIM.PL, MAJOR.R@IMIM.PL

Abstract

Biological functionalization is a critical area of research aimed at enhancing the functionality and application of biomaterials in various biomedical fields. One of the key aspects of biofunctionalization involves the addition of growth factors, which can significantly improve the biocompatibility of materials. Enhanced biocompatibility allows these materials to integrate more effectively with surrounding tissues, promoting their acceptance by the body and minimizing the risk of rejection or inflammation. This study is focused on investigations of the surface properties of polyelectrolyte layers, micelles, and complex systems utilizing red blood cells (RBCs) as carriers for growth factors. Through electrostatic interactions between negatively charged RBCs and positively charged polyelectrolytes, it becomes possible to modify red blood cells for use as effective delivery systems. Additionally, polyelectrolyte micelles can be employed for delivery purposes through grafting with suitable polymers. All of the tested surfaces exhibited hydrophilic characteristics, as indicated by measurements of the contact angle. Furthermore, the study determined the zeta potential of modified red blood cells and presented methods for the docking of vascular endothelial growth factor (VEGF) onto both RBCs and micelles. The obtained results highlight the potential of these biofunctionalized systems for improving therapeutic outcomes in regenerative medicine and drug delivery.

Keywords: drug delivery system, red blood cell (RBC), polyelectrolyte micelles, grafted copolymers

[Engineering of Biomaterials 172 (2024) 07]

doi:10.34821/eng.biomat.172.2024.07

Submitted: 2024-07-19, Accepted: 2024-08-14, Published: 2024-08-20



Copyright © 2024 by the authors. Some rights reserved.
Except otherwise noted, this work is licensed under
<https://creativecommons.org/licenses/by/4.0>

Introduction

Modern drug delivery systems can be divided into two groups - the first group consists of vehicles based on biological structures, such as viruses and cells, for example, red blood cells (RBCs) [1]. The second group includes artificially created carriers, such as micelles, capsules, and polymer complexes. In the case of artificially created drug delivery systems, particular attention is given to polyelectrolytes, which can form micellar structures and thin films, offering unique properties such as controlled drug release and surface modification capabilities. These systems can be tailored to meet specific therapeutic needs and various applications.

The interaction between a cell and a surface of a material is fundamental in the design process of an implant or biomaterial. In addition to ensuring essential material properties such as the absence of mutagenic and cytotoxic effects or the induction of inflammatory responses, it is crucial to understand the cellular mechanisms involved in the interaction between a cell and a surface in order to design a bioactive material [2]. The response of cells to a material is a complex process that is crucial for understanding many biological and medical phenomena.

When a cell comes into contact with a material, its first response is the attachment to the surface of the material. The cell membrane has a negative charge due to the presence of phospholipid bilayers, so the positively charged material can attract cells to its surface, thereby improving cell adhesion. The surface charge of the material also affects protein adsorption [3]. In the body, proteins from blood or other body fluids adhere first, even before cells attach to the material. To ensure the appropriate surface charge, materials with functional groups on their surface are used to promote protein adsorption. Modification with polyelectrolytes allows for changes in surface characteristics and tailoring them to the desired outcomes [4-6]. Polyelectrolytes, with their unique chemical properties, enable precise control over surface properties of materials, such as hydrophilicity, surface charge, and biocompatibility [7]. By using different types of polyelectrolytes and application techniques, the surface of materials can be tailored to specific requirements [8].

Polyelectrolytes can be applied for example using layer-by-layer technique. It is based on the alternate deposition of polyanions and polycations. As substrates, cleaned hydrophilic surfaces such as glass, which has a nonzero surface charge, can be used. The adsorption of the first layer is achieved by immersing the charged substrate into a solution containing a polyion of opposite charge. After a typical adsorption time of 8 minutes, the substrate is rinsed with NaCl to remove excess polymer. The adsorption of the polyion layer results in surface charge overcompensation, causing the net charge to reverse, which allows for the adsorption of a polyion with the opposite charge [7,9]. This method enables the formation of both polyelectrolyte films and micellar structures. In the case of micelles, amphiphilic polymers, such as polyelectrolytes, self-organize in solution, forming a structure with a hydrophobic core surrounded by a hydrophilic outer layer.

The process relies on the self-assembly of polymers based on their electrostatic and amphiphilic properties. A polyanion or polication can be either a homopolymer or a copolymer. Homopolymers are obtained by crosslinking only one type of small ion or monomer [8]. Copolymers are formed by crosslinking two different types of monomers. They are used to combine the desirable properties of different monomers, improving material characteristics such as mechanical strength, flexibility, and chemical resistance.

Copolymers can be tailored for specific functions, such as enhanced biocompatibility or controlled drug release. Additionally, they allow better control over properties such as solubility and processability, making them useful in various industrial and biomedical applications. An example of using a copolymer is with NIPAM (N-isopropylacrylamide), which is a thermoresponsive monomer [10]. When incorporated into a copolymer, NIPAM can be used to create materials that respond to temperature changes due to its unique thermoresponsive properties, as it undergoes a phase transition at a specific temperature of around 32°C.

Natural carriers, such as red blood cells, are gaining popularity due to their biocompatibility, biodegradability, and ability to circulate for extended periods in the body. RBCs can be utilized as carriers for various therapeutic agents, allowing controlled release. Drugs can be encapsulated within RBCs, allowing for controlled release and improved pharmacokinetics [11]. Additionally, through surface modification, RBCs can enhance the targeting of drugs to specific tissues, thereby increasing therapeutic efficacy and minimizing side effects. The erythrocyte cell membrane can also be utilized, as it can be coated with nanoparticles, enhancing their biocompatibility and targeting capabilities [12,13]. Despite these advancements, challenges remain in understanding the interactions between nanoparticles and RBCs, which could impact the efficacy of these delivery systems [4,7,14].

In this study, two types of drug delivery systems were prepared: one based on polyelectrolyte multilayers (PEM) and the other based on red blood cells (RBC). VEGF was incorporated into both systems and its influence on PEM and RBC surfaces was assessed through Zeta potential measurements, surface free energy, wettability, microstructure, and roughness analysis.

Materials and Methods

Synthesis of Chitosan-g-PNIPAM copolymers

1.0 g of chitosan (Chi) (448869, Sigma Aldrich) and 2.5 g of N-isopropylacrylamide (NIPAM) (412780025, Thermo Scientific Chemicals) were dissolved in 40 ml of a 10% aqueous acetic acid solution (568760114, POCH). The solution was purged with liquid nitrogen and heated to 40°C. The formulas used for synthesis were developed based on the literature [10]. Next, the 0.8 g cerium ammonium nitrate (CAN, Ce⁴⁺) (ACRS20144, POCH) was dissolved in 5 ml of distilled water and heated to 40°C before being added to the solution prepared in the first step. After the addition of CAN, the reaction was allowed to proceed for 4-6 h at 40°C. The resulting Chi-g-PNIPAM copolymer was separated from the PNIPAM homopolymer by pouring the reaction mixture into a large quantity of acetone for 24 h and filtering the reaction product (FIG. 1). The product was then subjected to extraction in acetone for 48 h and dried at room temperature.

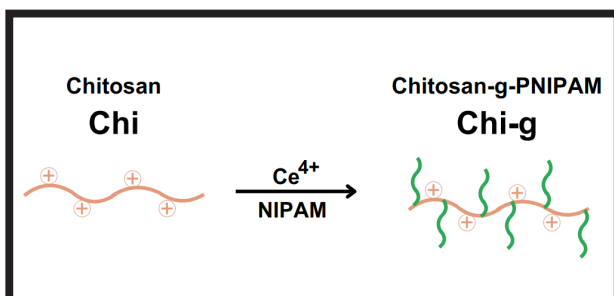


FIG. 1. Schematic representation of the formation of Chitosan-g-PNIPAM; orange for chitosan, green for PNIPAM.

Synthesis of Alginate-g-P(NIPAM-co-AA) copolymers

2.0 g sodium alginate (Alg) (180947, Sigma Aldrich), 1.5 g NIPAM and 0.5 g acrylic acid (AA) (181285, Sigma Aldrich) were dissolved in 30 ml ultrapure water. The formulas used for synthesis were developed based on the literature [15]. As the initiator of the redox system ammonium persulfate (09913, Sigma Aldrich) and sodium sulphite (71988, Sigma Aldrich) were utilized. 20 mg ammonium persulfate and 20 mg of sodium sulphite were separately dissolved, each in 1 ml of ultrapure water, then the solutions were added to the monomer solution. The polymerization was carried out at 25°C for 24 h following a nitrogen purge. The resulting product was soaked in a large volume of acetone and then filtered to eliminate the homopolymer (FIG. 2). Subsequently, the copolymers were extracted with methanol for 48 h and dried under vacuum at 30°C to yield ALG-g-P(NIPAM-co-AA).

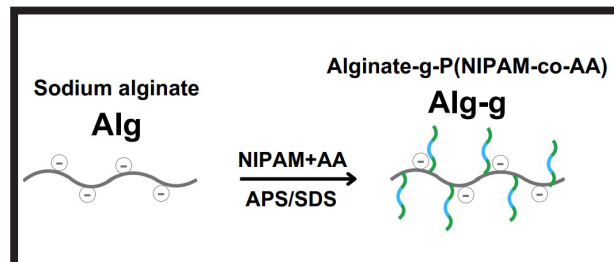


FIG. 2. Schematic representation of the formation of Alginate-g-P(NIPAM-co-AA); grey for alginate, green for PNIPAM, blue for acrylic acid.

VEGF Chitosan-g-PNIPAM

Chitosan-g-PNIPAM prepared as described in the previous chapter was dissolved at a concentration of 0.5 mg/ml. Vascular endothelial growth factor, originally known as vascular permeability factor (VPF), is a signal protein produced by many cells that stimulates the formation of blood vessels [16]. All members of the VEGF family stimulate cellular responses by binding to tyrosine kinase receptors (the VEGFRs) on the cell surface, causing them to dimerize and become activated through transphosphorylation, although to different sites, times, and extents [17]. VEGF (Gibco, PHC9394) solution in phosphate buffered saline (PBS) pH 7.4, containing 0.1% bovine serum albumin (BSA) was added to the prepared solution of grafted chitosan to reach a concentration of 20 ng/ml. The solution was placed at 4°C to absorb the VEGF and maintained in this state for 72 h (FIG. 3).

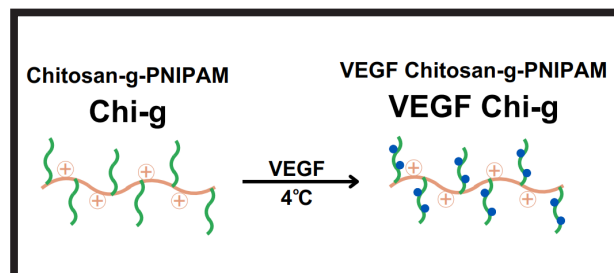


FIG. 3. Schematic representation of the formation of VEGF Chitosan-g-PNIPAM; orange for chitosan, green for PNIPAM, blue dots for VEGF.

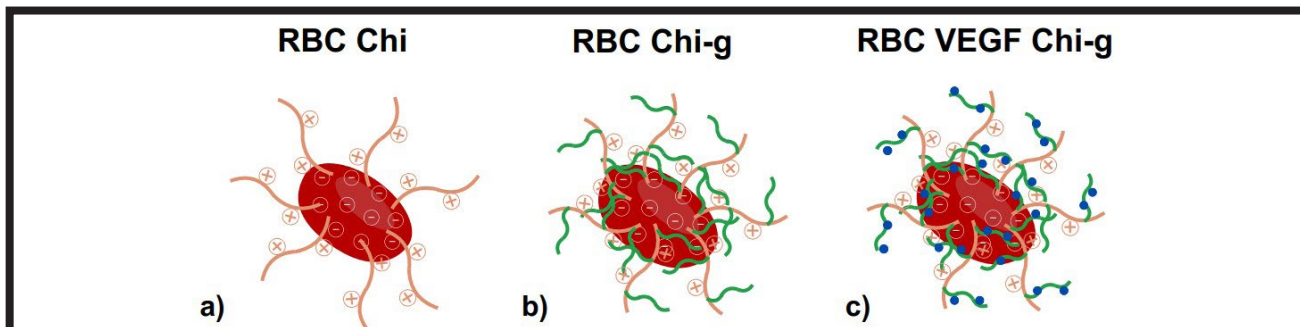


FIG. 4. Schematic representation of the formation of a) RBC with chitosan, b) RBC with chitosan-g-PNIPAM, c) RBC with VEGF chitosan-g-PNIPAM; orange for chitosan, green for PNIPAM, blue dots for VEGF.

Modifications of red blood cells

RBCs have a negative surface charge, and this property was utilized for VEGF delivery. Red blood cell concentrates were obtained from the Regional Blood Donation Centre. A single unit of red blood cell concentrate is derived from one unit of whole blood, after most of the plasma has been removed. It contains all red blood cells from the original unit of whole blood (with a hematocrit ranging from 0.65 to 0.75) and may also contain varying amounts of platelets and leukocytes, depending on the centrifugation process. Solutions of chitosan, grafted chitosan, and grafted chitosan with VEGF were prepared each at a concentration of 0.5 mg/ml. To 10 ml of each of these solutions, 40 μ l of erythrocyte concentrate was added (FIG. 4). The prepared solutions were used as the final positive layer applied after cross-linking the base sample.

Zeta potential analysis of red blood cells

Due to the strong surface charge on the erythrocytes membrane, they could be modified by electrostatic interaction. The surface was modified by chitosan, grafted chitosan, and grafted chitosan with VEGF as described in the previous paragraph. Cells with the modified surface were examined in terms of zeta potential.

A low ionic strength solution (LISS), containing 0.03 mol/L NaCl, was used as the medium in the study. 450 μ l of each chitosan solution was centrifuged for 5 min at 4000 rpm, the supernatant was then removed, and 1 ml of LISS was added to the resulting pellet. The measurements were carried out using electrophoretic light scattering (ELS) – a typical setup to assess zeta potential, widely used and reliable for biological and medical samples as well [18, 19]. Mixed-Mode Measurement phase analysis light scattering was performed on Malvern ZetaSizer Ultra (Malvern Panalytical, UK). This set up is equipped with 633 nm He-Ne laser beam of 10 mW power and an avalanche photodiode detector. For each measurement, 750 μ l of tested solution was placed in a PP DTS1070 capillary cuvette and then placed in the cuvette slot. For each sample, three repetitions were performed, with 25 measurements taken for each repetition. All proceedings were performed in a temperature equal to 25°C. Primary signal validity and analysis were done using ZS XPLOER software (version 3.3.1.5).

Polyelectrolyte multilayer films fabrication

Polyelectrolytes were applied by the layer-by-layer method, utilizing a robot that sequentially immerses the samples in solutions to deposit the layers (FIG. 5). A glass coverslip (14 x 14 mm) was used as the substrate.

Chitosan, chondroitin sulfate (PA-0306763-C, Pol-aura) and previously prepared grafted polymers were used in this study. The concentrations of used polyanions, polycations and copolymers are listed in TABLE 1. Each substance was dissolved in 5 M NaCl pH 7.4.

TABLE 1. List of polycations and polyanions.

Polyelectrolyte	Acronym	Charge	Concentration [mg/ml]
Chitosan	Chi	Positive	0.5
Chondroitin sulfate	CSu	Negative	1.0
Chitosan-g-PNIPAM	Chi-g	Positive	0.5
Alginate-g-P(NIPAM-co-AA)	Alg-g	Negative	1.0

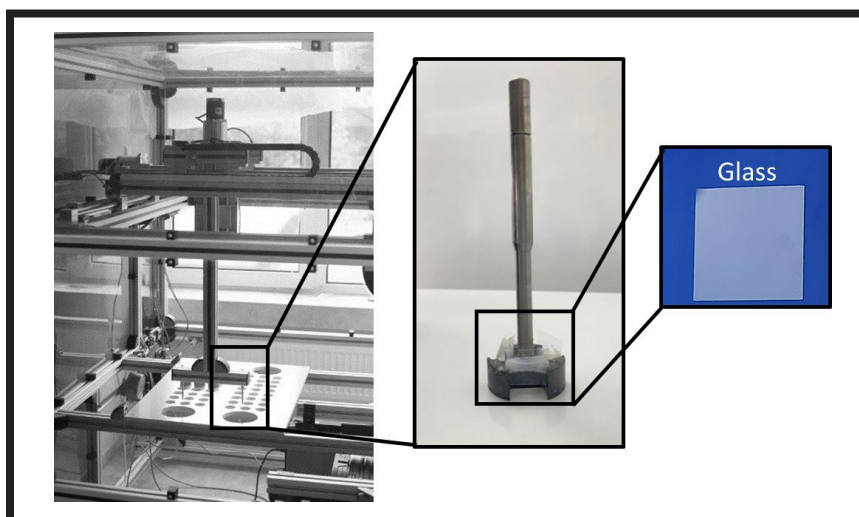


FIG. 5. Robot designed for applying polyelectrolyte layers along with a holder containing the samples. Authored and produced by Institute of Metallurgy and Materials Science, Polish Academy of Sciences.

TABLE 2. List of samples.

Number	Polycation	Polyanion	Crosslinking	Final layer
1	Chi-g	Alg-g	NHS/EDC	Chi-g
2	Chi-g	Alg-g	NHS/EDC	VEGF Chi-g
3	Chi-g	Alg-g	NHS/EDC - VEGF	Chi-g
4	Chi	CSu	NHS/EDC	RBC Chi
5	Chi	CSu	NHS/EDC	RBC Chi-g
6	Chi	CSu	NHS/EDC	RBC VEGF Chi-g

6 variants of coatings applied by "layer-by-layer" method were prepared. Initially, basic coatings Chi/CS and Chi-g/Alg-g were obtained. Subsequently, PEM with RBC was made, followed by PEM with the growth factor VEGF, which was docked to RBC and to micelles. The list of samples is presented in TABLE 2. All samples were crosslinked by applying EDC (1-ethyl-3-(3-dimethylaminopropyl)carbodiimide, 03449, Sigma Aldrich) and NHS (N-hydroxysuccinimide, 130672, Sigma Aldrich) for 24 h. The concentration of NHS was 22 mg/ml, and the concentration of EDC was 60 mg/ml. The crosslinking reagents were dissolved separately in 5 M NaCl, then combined right before being applied to the surface. For sample number 3, NHS/EDC was pre-mixed with VEGF to achieve a concentration of 20 ng/ml of VEGF.

After the designated time, the crosslinking reagent was removed, and a final layer was applied for 8 minutes to ensure that the surface charge was positive. Depending on the type of the samples, different types of reagents were applied as the final layer (TABLE 2). All prepared layers consisted of 12 bilayers. After preparation, the samples were stored in 5 M NaCl at 4°C and each sample was imaged using a confocal microscope to analyze its surface.

Surface wettability

To determine the contact angle, an optical goniometer, Drop Shape Analyzer DSA100 (KRÜSS, Germany), along with the DSA4 software, were used. The measurements were conducted using the sessile drop method. A drop of 1.5 μ l was deposited onto the material using a pipette. For each type of material and test liquid, ten repetitions of the measurement were performed. Distilled water and diiodomethane (0335000100, LOBA Chemie) were applied as polar and nonpolar test liquids, respectively. Distilled water was obtained from a Direct-Q 3 UV system, Merck Millipore, with a 0.22 μ m membrane filter (MPGP02001, Milli-Q). The surface free energy (SFE) was determined by using the average wetting angle value and the Owens-Wendt model [20].

Surface imaging and roughness measurement

The surface of the prepared samples was imaged using a confocal laser scanning microscope (Carl Zeiss CLSM Exciter 5) with 5x and 50x magnification. Roughness parameters were obtained using ConfoMap software in accordance with ISO 25178. For each modification, six images were taken, from which the average and standard deviation were calculated.

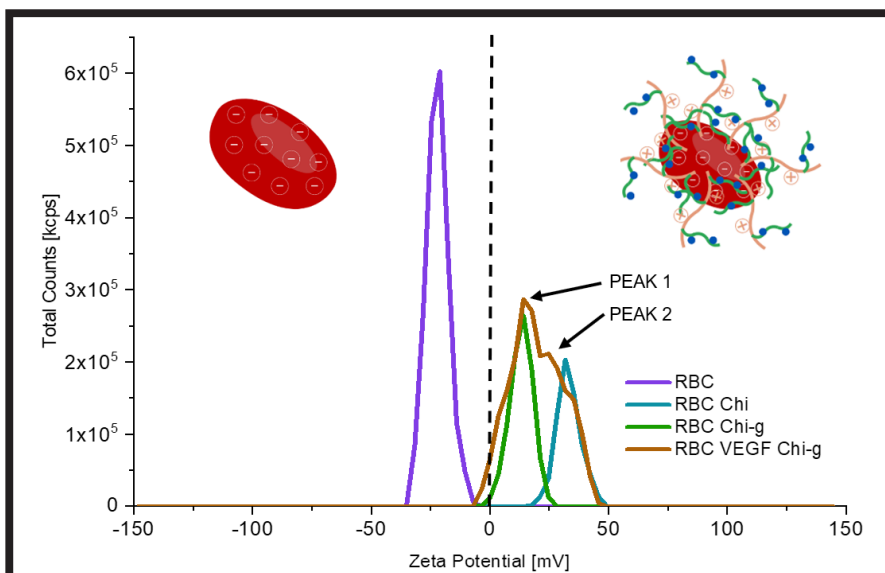
Results and Discussions

The determination of zeta potential

The distribution of zeta potential for all tested samples is presented in FIG. 6. The zeta potential of pure red blood cells is negative due to the presence of sialic acid residues on the glycoproteins. After adding the chitosan solution, which carries a positive charge due to the presence of amino groups, the red blood cells (RBCs) interact with the chitosan. These electrostatic interactions between the positively charged chitosan and the negatively charged RBCs leads to a change in the zeta potential, influencing RBCs stability and behaviour in the solution. For RBC modified with Chi-g-PNIPAM, the zeta potential is lower than for RBC with chitosan, but it remains positive, with an average zeta potential value of 11.53 (TABLE 3). It may be due to the presence of PNIPAM. For RBC with VEGF, two peaks were detected during the measurement – the first at 11.31 and the second at 24.57 (TABLE 3). This indicates the presence of two fractions that were detected in the measurement solution [21].

TABLE 3 Mean zeta potential (ζ) values of the measured particles.

Sample	Mean zeta potential [mV]	
RBC	-20.66	
RBC Chi	28.84	
RBC Chi-g-PNIPAM	11.53	
RBC Chi-g-PNIPAM VEGF	PEAK 1	11.31
	PEAK 2	24.57

FIG. 6. The distribution of zeta potential (ζ) of the RBCs and modified RBCs.

Confocal Laser Scanning Microscopy (CLSM)

The formation of aggregates in drug delivery systems can lead to uneven drug release and reduced bioavailability, diminishing therapeutic efficacy and increasing the risk of toxicity. Therefore, surface studies of the samples were conducted to determine the uniformity of substrate coverage by the prepared modifications. The surfaces of the samples are presented in FIG. 7 and FIG. 8.

The samples were visualized using Confocal Laser Scanning Microscopy in the transmitted light mode. For the sample where VEGF was applied along with the crosslinking agent, a change in the surface smoothness of the sample is evident (FIG. 7c,d), as compared to the sample where VEGF was added as the last layer. In all of the samples, a uniform arrangement of micelles across the entire surface of the sample is observed. No localized clusters or aggregations were noted, indicating good coating quality.

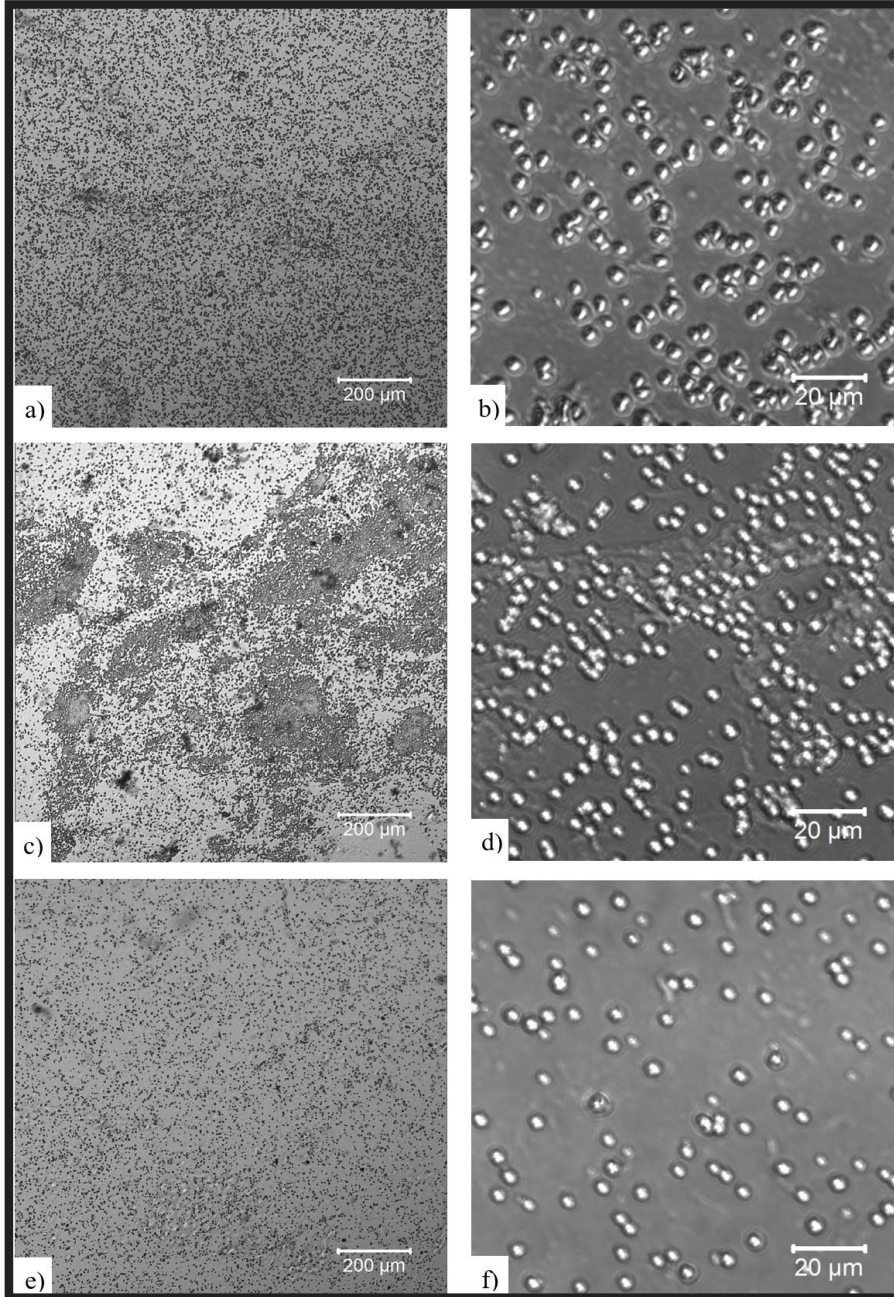


FIG. 7. Polyelectrolytes complex micelles; CLSM magnification 5x:
 a) $(\text{Chi-g/Alg-g})_{12}$,
 c) $(\text{Chi-g/Alg-g})_{12}$ VEGF,
 e) $(\text{Chi-g-VEGF/Alg-g})_{12}$,
CLSM magnification 50x:
 b) $(\text{Chi-g/Alg-g})_{12}$,
 d) $(\text{Chi-g/Alg-g})_{12}$ VEGF,
 f) $(\text{Chi-g-VEGF/Alg-g})_{12}$.

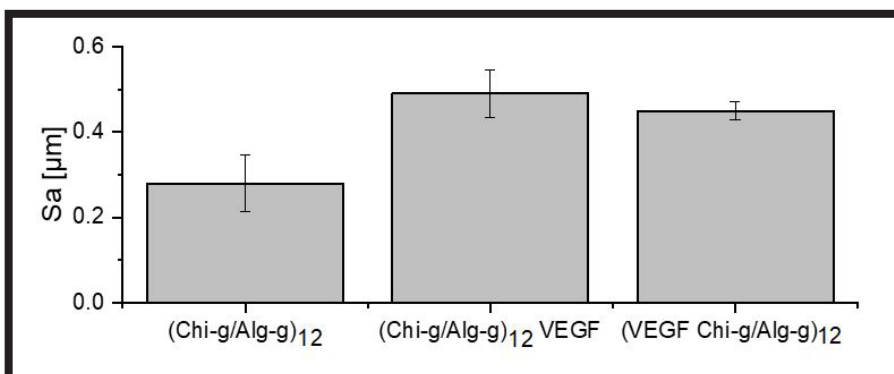


FIG. 8. Surface roughness of sample with polyelectrolytes complex micelles.

In FIG. 9, the roughness parameter of the substrate is presented, specifically the Sa parameter (arithmetical mean height). This parameter is generally used to evaluate surface roughness. The (Chi-g/Alg-g)₁₂ VEGF sample exhibited the highest roughness value among the micelles, equal to 0.49 μm .

For the samples where the last layer consisted of modified erythrocytes, the presence of two particle sizes can be observed, with one being the modified erythrocytes and the other resembling micelle structures. Similar to the micelles, the layer applied here is uniform, and the erythrocytes did not form localized clusters (FIG. 9). The roughness for all RBC samples is the same, with values ranging from 0.26 to 0.31 μm , taking into account the standard deviation (FIG. 10).

The presented drug delivery systems have potential applications in various biomedical fields. If utilized as a coating for bone implants, the increased surface roughness could enhance the attachment and proliferation of osteoblasts, which are essential for bone regeneration and implant integration [22]. In studies conducted by various researchers, it has been demonstrated that particles ranging in size from 1-3 μm can also be internalized by cells [23]. This finding is significant because it challenges the conventional understanding that particles larger than 150 nm cannot enter non-phagocytic cells via nonspecific endocytosis. Therefore, it is essential to conduct further research on the impact of our coating systems on cells to determine how these larger particles behave in a biological context. This will provide valuable insights into their potential in drug delivery or other biomedical applications.

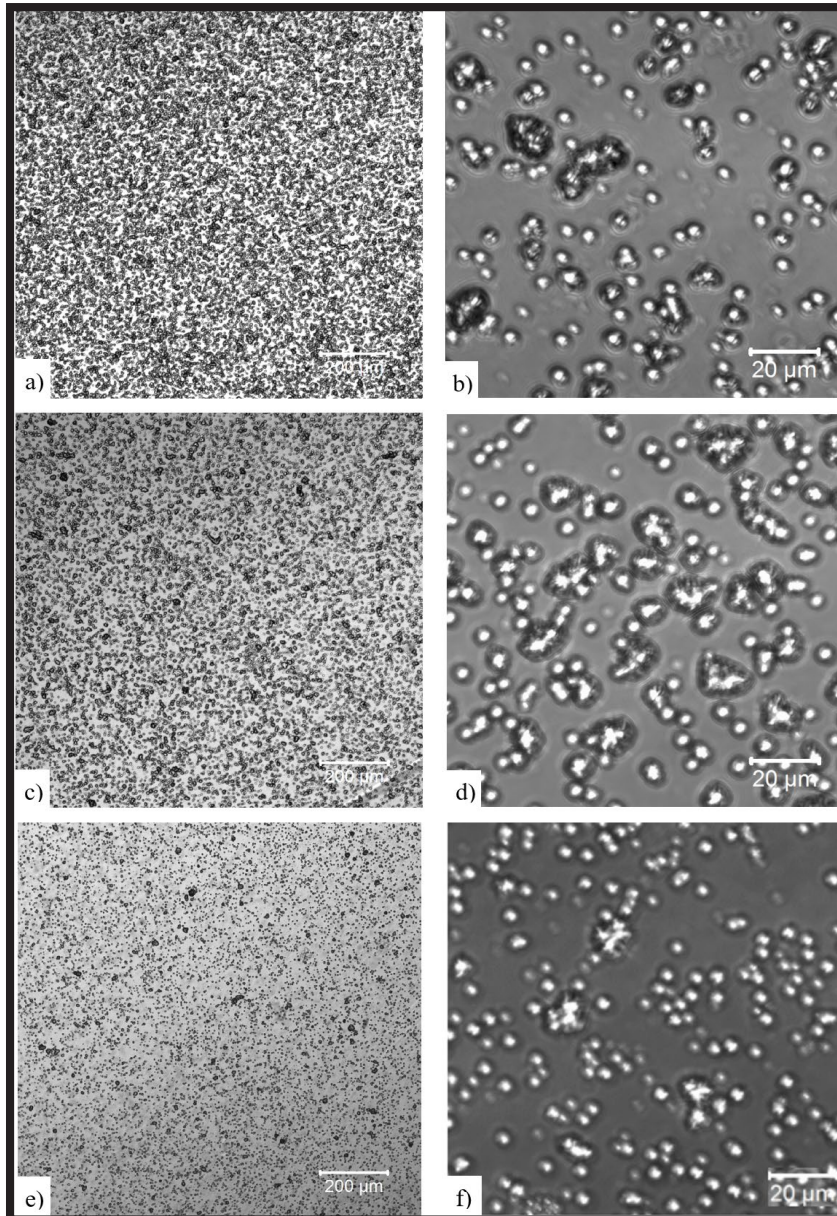


FIG. 9. Polyelectrolytes (Chi/CSu)₁₂ modified with red blood cells (RBCs), CLSM magnification 5x, finishing layer:
 a) RBC Chi,
 c) RBC Chi-g,
 e) RBC Chi-g-VEGF,
CLSM magnification 50x, finishing layer:
 b) RBC Chi,
 d) RBC Chi-g,
 f) RBC VEGF Chi-g.

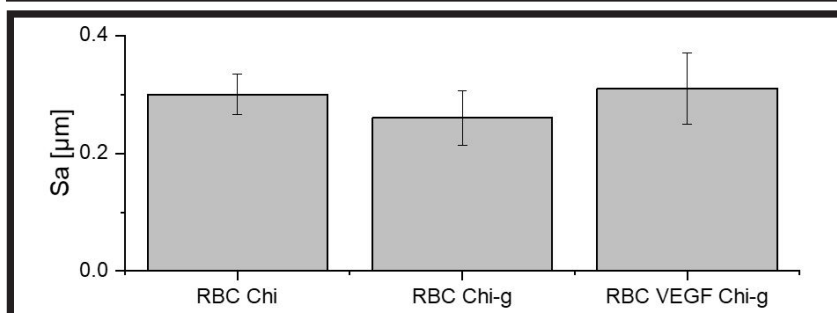


FIG. 10. Surface roughness of polyelectrolytes (Chi/CSu)₁₂ modified with red blood cells (RBCs).

TABLE 4. Components of SFE by the Owens-Wendt model and contact angle for polyelectrolytes complex micelles.

Polyelectrolytes complex micelles	Components of surface free energy [mJ/m ²]			Contact angle [°]	
	γ_s	γ_s^d	γ_s^p	Distilled water	Diiodomethane
(Chi-g/Alg-g) ₁₂	30.66	30.57	0.09	58.30 ± 5.80	56.50 ± 6.60
(Chi-g/Alg-g) ₁₂ VEGF	33.67	33.62	0.05	81.90 ± 9.20	51.20 ± 8.50
(VEGF Chi-g/ Alg-g) ₁₂	31.37	31.32	0.05	83.80 ± 5.60	55.20 ± 5.20

TABLE 5. Components of SFE by the Owens-Wendt model and contact angle for the sample with different final layer.

Final layer	Components of surface free energy [mJ/m ²]			Contact angle [°]	
	γ_s	γ_s^d	γ_s^p	Distilled water	Diiodomethane
RBC Chi	31.44	31.39	0.05	83.00 ± 7.00	55.10 ± 6.30
RBC Chi-g	32.73	32.67	0.06	75.70 ± 5.50	52.90 ± 8.90
RBC VEGF Chi-g	27.71	27.62	0.09	65.00 ± 7.60	61.70 ± 5.60

Contact angle measurement

Wettability plays a crucial role in the process of proteins and other macromolecules adsorption onto surfaces, bacterial adhesion and biofilm formation, as well as interactions between implants, drug carriers and the human body [24]. The sample (Chi-g/Alg-g)₁₂ was shown to have the smallest water contact angle for distilled water (58.3°), indicating the highest hydrophilicity among the analyzed polyelectrolyte complex micelles (TABLE 4). The introduction of VEGF in the (Chi-g/Alg-g)₁₂ VEGF and (VEGF Chi-g /Alg-g)₁₂ samples resulted in an increase in the contact angle, indicating a decrease in surface hydrophilicity. The addition of VEGF altered the hydrophobic properties of the surface, which was reflected in the higher water contact angles, particularly in the (Chi-g/Alg-g)₁₂ VEGF sample. For diiodomethane, the differences between the samples were less pronounced compared to the results for water and fell within the range of the standard deviation. The introduction of VEGF resulted in an increase in total surface energy (TABLE 4), which could indicate enhanced surface reactivity in interactions with the human body's environment. However, these changes did not significantly affect the polar component, indicating that the surfaces were still dominated by dispersive (van der Waals) interactions. It is possible that VEGF has modified the nature of interactions on the material's surface.

The results of the contact angle measurements for the samples with erythrocytes are shown in TABLE 5. The RBC Chi sample with the final layer displayed the highest contact angle for distilled water at 83.0° (TABLE 5), indicating it was the most hydrophobic among all RBC samples. The introduction of the Chi-g and VEGF Chi-g modifications led to a decrease in contact angle values, which means an increase in surface hydrophilicity. This was especially evident in the case of the RBC VEGF Chi-g sample, which exhibited the lowest contact angle (65.0°), indicating that the surface became the most hydrophilic in this series of samples. For all RBC samples, it was observed that the dispersive component constituted almost the entire surface free energy (SFE), meaning that dispersive forces (van der Waals) dominated surface interactions (TABLE 5).

The polar component was small, ranging from 0.05 to 0.09, indicating that the surfaces had minimal polar character and were unlikely to interact well with polar substances. The introduction of VEGF in the RBC VEGF Chi-g sample resulted in a reduction in total SFE, which suggested that the surface became more stable comparing to the another sample with RBCs. Dispersive and hydrophobic surfaces can limit the adhesion of proteins or cells compared to surfaces with stronger polar components, which can affect biocompatibility and the effectiveness of performance of tested materials. For implants, it is crucial to tailor the surface to specific biological requirements to ensure desirable interactions. In studies [25], poly(L-lactic acid) (PLLA) films were used as drug delivery systems, exhibiting water contact angles ranging from 50 to 80, which is comparable to the values obtained in our experiments.

Conclusions

The results obtained in this study demonstrate that the modified erythrocytes are stable in aqueous solution. Due to their negative surface charge, they have the potential to serve as effective vehicles for drug delivery. Additional research is required to gain further insights into the two fractions identified during the ELS study of VEGF Chi-g-PNIPAM-modified erythrocytes. Wettability tests confirmed that the polyelectrolytes, in both layered and micellar forms, are hydrophilic, making them suitable for cell culture applications. Furthermore, the surface characteristics of the obtained samples are well-developed, which can promote cell attachment and proliferation.

Acknowledgements

The work was funded by the project of the National Science Centre, decision no. 2022/47/O/ST5/02102 "Porous materials produced from ice templates dedicated to endothelial-muscle cell coculture".

References

- [1] S. Tan, T. Wu, D. Zhang, Z. Zhang: Cell or Cell Membrane-Based Drug Delivery Systems. *Theranostics* 5 (2015) 863-881. <https://doi.org/10.7150/thno.11852>.
- [2] H. Amani, H. Arzaghi, M. Bayandori, A.S. Dezfouli, H. Pazoki-Toroudi, A. Shafiee, L. Moradi: Controlling Cell Behavior through the Design of Biomaterial Surfaces: A Focus on Surface Modification Techniques. *Adv Mater Interfaces* 6 (2019). <https://doi.org/10.1002/admi.201900572>.
- [3] E.Y. Xi Loh, M.B. Fauzi, M.H. Ng, P.Y. Ng, S.F. Ng, H. Ariffin, M.C.I. Mohd Amin: Cellular and Molecular Interaction of Human Dermal Fibroblasts with Bacterial Nanocellulose Composite Hydrogel for Tissue Regeneration. *ACS Appl Mater Interfaces* 10 (2018) 39532-39543. <https://doi.org/10.1021/acsami.8b16645>.
- [4] L.-M. Petrila, F. Bucatariu, M. Mihai, C. Teodosiu: Polyelectrolyte Multilayers: An Overview on Fabrication, Properties, and Biomedical and Environmental Applications. *Materials* 14 (2021) 4152. <https://doi.org/10.3390/ma14154152>.
- [5] D.F. Williams: Biocompatibility pathways and mechanisms for bioactive materials: The bioactivity zone. *Bioact Mater* 10 (2022) 306-322. <https://doi.org/10.1016/j.bioactmat.2021.08.014>.
- [6] J. Saqib, I.H. Aljundi: Membrane fouling and modification using surface treatment and layer-by-layer assembly of polyelectrolytes: State-of-the-art review. *Journal of Water Process Engineering* 11 (2016) 68-87. <https://doi.org/10.1016/j.jwpe.2016.03.009>.
- [7] C. Picart: Polyelectrolyte Multilayer Films: From Physico-Chemical Properties to the Control of Cellular Processes. *Curr Med Chem* 15 (2008) 685-697. <https://doi.org/10.2174/092986708783885219>.
- [8] V.S. Meka, M.K.G. Sing, M.R. Pichika, S.R. Nali, V.R.M. Kolapalli, P. Kesharwani: A comprehensive review on polyelectrolyte complexes. *Drug Discov Today* 22 (2017) 1697-1706. <https://doi.org/10.1016/j.drudis.2017.06.008>.
- [9] M. Schönhoff: Layered polyelectrolyte complexes: physics of formation and molecular properties. *Journal of Physics: Condensed Matter* 15 (2003) R1781-R1808. <https://doi.org/10.1088/0953-8984/15/49/R01>.
- [10] M. Qi, G. Li, N. Yu, Y. Meng, X. Liu: Synthesis of thermo-sensitive polyelectrolyte complex nanoparticles from CS-g-PNIPAM and SA-g-PNIPAM for controlled drug release. *Macromol Res* 22 (2014) 1004-1011. <https://doi.org/10.1007/s13233-014-2134-6>.
- [11] P.M. Glassman, C.H. Villa, A. Ukidve, Z. Zhao, P. Smith, S. Mitragotri, A.J. Russell, J.S. Brenner, V.R. Muzykantor: Vascular Drug Delivery Using Carrier Red Blood Cells: Focus on RBC Surface Loading and Pharmacokinetics. *Pharmaceutics* 12 (2020) 440. <https://doi.org/10.3390/pharmaceutics12050440>.
- [12] L. Rossi, F. Pierigè, M.P. Aliano, M. Magnani: Ongoing Developments and Clinical Progress in Drug-Loaded Red Blood Cell Technologies. *BioDrugs* 34 (2020) 265-272. <https://doi.org/10.1007/s40259-020-00415-0>.
- [13] A. Vincy, S. Mazumder, Amrita, I. Banerjee, K.C. Hwang, R. Vankayala: Recent Progress in Red Blood Cells-Derived Particles as Novel Bioinspired Drug Delivery Systems: Challenges and Strategies for Clinical Translation. *Front Chem* 10 (2022). <https://doi.org/10.3389/fchem.2022.905256>.
- [14] R. Major, J.M. Lackner, M. Sanak, B. Major: Biomimetics in thin film design: Niche-like wrinkles designed for i-cell progenitor cell differentiation. *Materials Science and Engineering: C* 80 (2017) 379-386. <https://doi.org/10.1016/j.msec.2017.06.005>.
- [15] G. Li, S. Song, T. Zhang, M. Qi, J. Liu: pH-sensitive polyelectrolyte complex micelles assembled from CS-g-PNIPAM and ALG-g-P(NIPAM-co-NVP) for drug delivery. *Int J Biol Macromol* 62 (2013) 203-210. <https://doi.org/10.1016/j.ijbiomac.2013.08.041>.
- [16] D.R. Senger, S.J. Galli, A.M. Dvorak, C.A. Perruzzi, V.S. Harvey, H.F. Dvorak: Tumor Cells Secrete a Vascular Permeability Factor That Promotes Accumulation of Ascites Fluid. *Science* 219 (1983) 983-985. <https://doi.org/10.1126/science.6823562>.
- [17] K. Holmes, O.L. Roberts, A.M. Thomas, M.J. Cross: Vascular endothelial growth factor receptor-2: Structure, function, intracellular signalling and therapeutic inhibition. *Cell Signal* 19 (2007) 2003-2012. <https://doi.org/10.1016/j.cellsig.2007.05.013>.
- [18] H.P. Fernandes, C.L. Cesar, M. de L. Barjas-Castro: Electrical properties of the red blood cell membrane and immunohematological investigation. *Rev Bras Hematol Hemoter* 33 (2011) 297-301. <https://doi.org/10.5581/1516-8484.20110080>.
- [19] F. Tokumasu, G.R. Ostera, C. Amaratunga, R.M. Fairhurst: Modifications in erythrocyte membrane zeta potential by Plasmodium falciparum infection. *Exp Parasitol* 131 (2012) 245-251. <https://doi.org/10.1016/j.exppara.2012.03.005>.
- [20] S. Łagan, A. Chojnacka-Brozek, A. Liber-Kneć, G. Malik: Surface free energy and roughness of flowable dental composites. *Acta Bioeng Biomech* 25 (2023). <https://doi.org/10.37190/ABB-02306-2023-02>.
- [21] S.Z. Alshawwa, A.A. Kassem, R.M. Farid, S.K. Mostafa, G.S. Labib: Nanocarrier Drug Delivery Systems: Characterization, Limitations, Future Perspectives and Implementation of Artificial Intelligence. *Pharmaceutics* 14 (2022) 883. <https://doi.org/10.3390/pharmaceutics14040883>.
- [22] P. Kurtyka, M. Kopernik, M. Kaczmarek, M. Surmiak, Ł. Major, R. Kustos, J. Więcek, K. Kurtyka, A. Bartkowiak, R. Major: Biofunctional impact of textured coatings in the application of heart assist therapy. *Archives of Civil and Mechanical Engineering* 23 (2022) 31. <https://doi.org/10.1007/s43452-022-00573-8>.
- [23] S.E.A. Gratton, P.A. Ropp, P.D. Pohlhaus, J.C. Luft, V.J. Madden, M.E. Napier, J.M. DeSimone: The effect of particle design on cellular internalization pathways. *Proceedings of the National Academy of Sciences* 105 (2008) 11613-11618. <https://doi.org/10.1073/pnas.0801763105>.
- [24] R.A. Gittens, L. Scheideler, F. Rupp, S.L. Hyzy, J. Geis-Gerstorfer, Z. Schwartz, B.D. Boyan: A review on the wettability of dental implant surfaces II: Biological and clinical aspects. *Acta Biomater* 10 (2014) 2907-2918. <https://doi.org/10.1016/j.actbio.2014.03.032>.
- [25] M. Behnecke, S. Petersen: Establishment of PEEK-Associated Drug Delivery Systems - Limits and Perspectives. *Journal of Materials Science and Chemical Engineering* 08 (2020) 32-41. <https://doi.org/10.4236/msce.2020.810004>.